New horizons in cardiac innervation imaging: introduction of novel ^{18}F-labeled PET tracers

Ryohei Kobayashi[1,2] · Xinyu Chen[1,3] · Rudolf A. Werner[1,3,4] · Constantin Lapa[1] · Mehrbod S. Javadi[4] · Takahiro Higuchi[1,3,5]

Abstract Cardiac sympathetic nervous activity can be uniquely visualized by non-invasive radionuclide imaging techniques due to the fast growing and widespread application of nuclear cardiology in the last few years. The norepinephrine analogue ^{123}I–meta-iodobenzylguanidine (^{123}I–MIBG) is a single photon emission computed tomography (SPECT) tracer for the clinical implementation of sympathetic nervous imaging for both diagnosis and prognosis of heart failure. Meanwhile, positron emission tomography (PET) imaging has become increasingly attractive because of its higher spatial and temporal resolution compared to SPECT, which allows regional functional and dynamic kinetic analysis. Nevertheless, wider use of cardiac sympathetic nervous PET imaging is still limited mainly due to the demand of costly on-site cyclotrons, which are required for the production of conventional ^{11}C-labeled (radiological half-life, 20 min) PET tracers. Most recently, more promising ^{18}F-labeled (half-life, 110 min) PET radiopharmaceuticals targeting sympathetic nervous system have been introduced. These tracers optimize PET imaging and, by using delivery networks, cost less to produce. In this article, the latest advances of sympathetic nervous imaging using ^{18}F-labeled radiotracers along with their possible applications are reviewed.

Keywords Heart failure · Sympathetic nervous system · Nuclear cardiology · SPECT · PET · ^{18}F-labeled radiotracer

Introduction

Understanding of the cardiac sympathetic nervous system has been expanded in the last decade, particularly as a relevant imaging target in patients with chronic heart failure (HF). HF is characterized by a vicious cycle, in which reduced cardiac output via myocardial injury results in sympathetic nerve hyperactivation that in turn causes further myocardial damage and reduction of cardiac performance [1]. Currently, improved mortality rates of chronic HF patients using therapeutic sympathetic nerve blockade has been confirmed [2–4]. Therefore, non-invasive monitoring of the individual cardiac sympathetic nervous status provides a powerful prognosis prediction tool, as well as optimizes therapeutic algorithms in order to harvest the greatest benefit of medical interventions. At present, nuclear medicine imaging techniques—including single-photon emission computed tomography (SPECT) and positron emission tomography (PET)—involving the application of very small amounts of radiopharmaceuticals/radiolabeled tracers are the only ways to evaluate the function of the cardiac sympathetic nervous system. In contrast to traditional imaging techniques (e.g. computed tomography and magnetic resonance imaging) that mainly present morphological information, PET or SPECT provides unique and crucial details at a subcellular to molecular level and thus has the potential to determine early onset of cardiac disease [5].

Ryohei Kobayashi and Xinyu Chen contributed equally to this article.

✉ Takahiro Higuchi
thiguchi@me.com

[1] Department of Nuclear Medicine, University Hospital of Würzburg, Oberdürrbacher Strasse 6, 97080 Würzburg, Germany

[2] Research Centre, Nihon Medi-Physics Co., Ltd., Chiba, Japan

[3] Comprehensive Heart Failure Center, University Hospital of Würzburg, Würzburg, Germany

[4] The Russell H Morgan Department of Radiology and Radiological Sciences, Johns Hopkins School of Medicine, Baltimore, MD, USA

[5] Department of Biomedical Imaging, Research Institute, National Cerebral and Cardiovascular Center, Suita, Japan

Norepinephrine analogue tracers, such as the SPECT tracer ^{123}I–meta-iodobenzylguanidine (^{123}I–MIBG, Fig. 1), provide integral information on myocardial sympathetic innervation and the nerve status at diagnosis [6–9]. In the sympathetic nervous system, the neurotransmitter norepinephrine (Fig. 1) is synthesized and stored in vesicles in presynaptic cells and is released into the synaptic cleft where it binds to postsynaptic adrenoreceptors to achieve neurotransmission and to trigger further downstream cascades. Norepinephrine in the synaptic cleft is then carried into the cells again by the norepinephrine transporters (NET) and stored in vesicles in the presynaptic nerve terminal for either re-use (so-called uptake-1 mechanism) or decomposition [9, 10]. In the same manner, but after intravenous administration, synthesized norepinephrine analogue tracers are taken up in nerve terminals actively via the uptake-1 mechanism. Therefore, localization of the tracer accumulation represents primarily sympathetic innervation—a key factor to assess the status of cardiac condition. The possible mechanisms of decreased tracer uptake and/or increased tracer washout include impaired NET function, sympathetic hyperactivation, and impaired vesicular storage function [6, 11, 12].

Advances in sympathetic nervous imaging

^{123}I–MIBG has been the most widely used clinical tracer for sympathetic nervous imaging for more than 30 years [13]. The potential application of MIBG as a prognostic parameter of HF was first described by Merlet et al. [14] in 1992 followed by several trials [12, 15, 16]. The subsequent landmark ADMIRE-HF (AdreView Myocardial Imaging for Risk Evaluation in Heart Failure) study has established the prognostic significance of ^{123}I–MIBG in HF patients and has confirmed that a lower H/M ratio from planar ^{123}I–MIBG imaging is strongly associated with a higher incidence of cardiac events [17]. Most recently, Nakajima et al. created risk charts for short-term (2 years) and long-term (5 years) prediction of cardiac risk using ^{123}I–MIBG H/M ratio based on the database of 1322 HF patients. The risk prediction models with ^{123}I–MIBG showed incremental prognostic value when compared with the model using only B-type natriuretic peptide (BNP) levels [18].

In addition, based on a study involving 106 patients, ^{123}I–MIBG washout rate is independently associated with sudden cardiac death (SCD) [19]. Although it is proven that implantable cardioverter defibrillators (ICD) reduce the risk of overall mortality and SCD in patients with congestive HF, the average annual rate of appropriate ICD shocks was only 5.1% [20]. Further studies proved the significance of including ^{123}I–MIBG scoring in the decision making of treating HF patients with ICD instead of only relying on LVEF [21, 22]. The clinical phase IIIb trial (ADMIRE-ICD), a multi-centre randomized clinical study, is currently in progress to demonstrate the clinical value of ^{123}I–MIBG imaging in appropriate decision-making of potential implantation in HF patients [23].

Parallel to SPECT tracers, several ^{11}C-labeled norepinephrine analogue tracers are also available. They show different uptake-1 affinity, stability on vesicular storage, and susceptibility to enzymatic degradation [24]. The studies using a combination of ^{11}C–epinephrine (EPI), ^{11}C–phenylephrine (PHEN), and ^{11}C–hydroxyephedrine (HED) revealed characteristic distributions and retentions of these tracers in myocardium of porcine and human subjects, reflecting presynaptic cardiac conditions in different ways [25, 26].

^{11}C–HED is so far the most routinely used PET tracer for sympathetic nervous imaging and has made a contribution to more profound understanding of pathogenesis and progression of HF [24, 27]. One of the recent studies suggested that ^{11}C–HED parameter can identify the beneficial impact of continuous positive airway pressure (CPAP) therapy in patients with obstructive sleep apnea (OSA, one of the common complications of heart disease) and HF with reduced ejection fraction (HFrEF) [28]. Subjects receiving short-term (6–8 weeks) CPAP therapy had increased myocardial ^{11}C–HED retention, while other cardiac parameters did not change.

Regional sympathetic denervation indicated by reduced myocardial ^{11}C–HED uptake was the strongest predictor of sudden cardiac arrest in a prospective study including 204 ischemic cardiomyopathy subjects. The subject group with

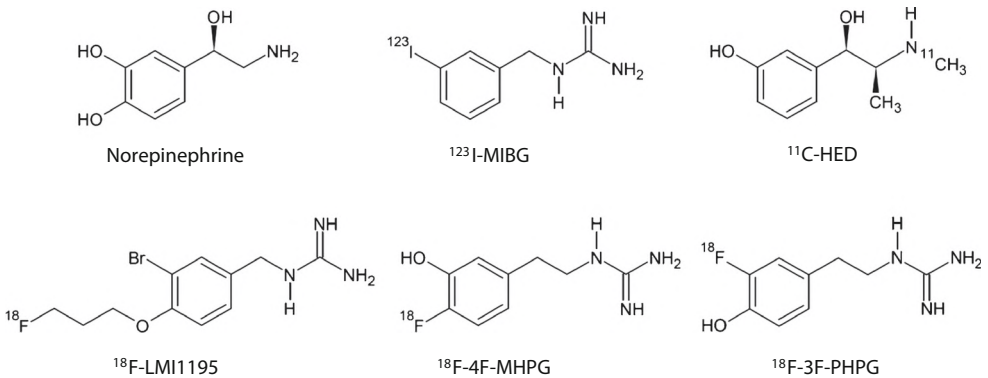

Fig. 1 Chemical structures of a radiolabeled neurotransmitter and neurotransmitter analogues

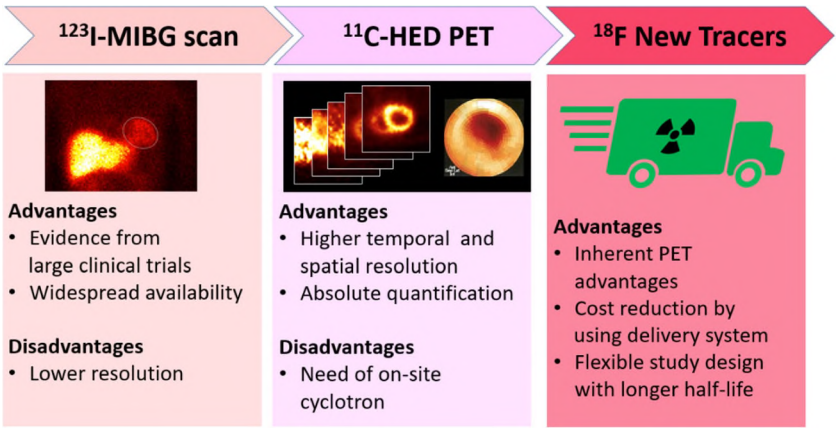

Fig. 2 ^{18}F-labeled PET tracers for sympathetic nervous imaging has promising characteristics for clinical practice with inherent high performance PET technology and potential of tracer cost reduction by using delivery system

the largest extent of reduced ^{11}C–HED uptake had a rate of sudden cardiac arrest of 6.7%/year, while the subject groups with intermediate and the smallest extent showed rates of 2.2%/year and 1.2%/year, respectively [29]. A study reported last year has also confirmed the direct correlation between low ^{11}C–HED retention and poor survival rate [30].

Introduction of novel ^{18}F-labeled sympathetic neuronal PET tracers

Despite many advantages, broader clinical application of conventional ^{11}C-labeled PET tracers, such as ^{11}C–HED, are quite limited mainly due to the short radiological half-life of only 20 min; thus, expensive and inflexible on-site cyclotrons for tracer production are mandatory (Fig. 2). This increases the financial burden for patients, as well as for small hospitals including both equipment and maintenance costs. In addition, this short half-life also strongly limits the novel tracer design for radiopharmacists. In contrast, ^{18}F-labeled tracers have a longer half-life (110 min), which allows the dispatch from central cyclotron facilities. This mode has already been established for ^{18}F–fluorodeoxyglucose (FDG) and has been proven to be cost-effective [31]. ^{18}F allows higher flexibility in designing and synthesizing novel PET tracers with more complex structures but more promising efficacy. Moreover, by introducing fluoride into tracers, it is possible to maintain the in vivo activity and selectivity towards specific targets, as well as to improve the stability against metabolism at sensitive position. Therefore, new perspectives include the development and application of ^{18}F-labeled radioligands that can use the full potential of PET technology. Recently, ^{18}F–LMI1195 and ^{18}F–4F-MHPG (Fig. 1) have been introduced and presented favorable properties for cardiac sympathetic nerve imaging. Preclinical development status of ^{18}F-labeled tracers is summarized in Table 1.

^{18}F–LMI1195

^{18}F–LMI1195 is so far the only tracer that has entered a phase I clinical trial, and the tracer profile is evaluated in most detail. Similar to ^{123}I–MIBG, ^{18}F–LMI1195 has a benzylguanidine-based structure and is not a substrate for metabolic degradation by cytosolic monoamine oxidase (MAO). Radiosynthesis of ^{18}F–LMI1195 can be achieved with a single-step ^{18}F replacement reaction. This timesaving, simplified radiolabeling procedure will be an advantage for commercialization in the near future.

Initial in vitro studies confirmed that ^{18}F–LMI1195 is avidly taken up via uptake-1 mechanism similar to endogenous norepinephrine [32]. Additionally, high specificity to uptake-1 mechanism was indicated by in vitro pharmacologic blocking studies using desipramine (around 90%)—a selective uptake-1 mechanism inhibitor [33]. This uptake-1 specific mechanism was verified in a subsequent study using isolated rabbit hearts. In this system, first-pass ^{18}F–LMI1195 extraction decreased flow-dependently, which suggests that^{18}F–LMI1195 initial uptake partially depends on the tracer quantity in the extracellular spaces that is limited by blood flow [34]. However, ^{18}F–LMI1195 appears to be more dependent on sympathetic innervation status than blood flow. In a denervated rabbit model, ^{18}F–LMI1195 was initially taken up in both normal and denervated areas in the first 2 min and afterwards rapidly washed out. This indicates higher rate constant for washout from extracellular space back to plasma (k2) than the rate constant for NET transportation (k3) [33].

After being taken up into presynaptic cells, ^{18}F–LMI1195 is thought to be stored predominantly in synaptic vesicles instead of a cytosol-dependent storage. As has been proved in isolated rabbit heart, the washout rate of ^{18}F–LMI1195 increased nearly three times when vesicular release from nerve terminals was enhanced by electrical field stimulation [34]. Although ^{123}I–MIBG, ^{11}C–HED, and ^{18}F–LMI1195 are all norepinephrine analogues and designed to mimic physiologic norepinephrine behavior, these tracers demonstrated distinct

Table 1 Preclinical development status of ^{18}F-labeled PET tracers targeting sympathetic nervous system

	In vitro study	Biodistribution study	Pharmacologic blocking study	PET imaging	Metabolite analysis	Human study
^{18}F–LMI1195	Human cell line [32, 33] Isolated rabbit heart [34]	Rat [32, 35, 36] Rabbit [32, 35]	Human cell line [33] Isolated rabbit heart [34] Rat [35, 37] Rabbit [32, 35, 38] Cynomolgus monkey [32]	Rat [32, 35, 37] Rabbit [32–35, 38] Cynomolgus monkey [32, 35]	Human [39]	Phase I [39]
^{18}F–4F-MHPG	Isolated rat heart (uptake-2 blocked) [40, 41]	Rat [40, 41]	Rhesus Macaque monkey [40, 41]	Rhesus macaque monkey [40, 41]	Rhesus macaque monkey [41], human [42]	Exploratory IND Study [42]
^{18}F–3F-PHPG	Isolated rat heart (uptake-2 blocked) [43]			Rhesus macaque monkey [43]	Rhesus macaque monkey [43], human [42]	Exploratory IND Study [42]
^{18}F–FPOIBG	Human cell line [44]	Mouse [44]	Human cell line [44] Mice [44]			
6-^{18}F-FMR		Rat [45–48] Dog [47, 48]	Rat [45, 47, 48] Dog [45]	Dog [45, 47]	Rat, Dog, Pig, Baboon [49]	
4-^{18}F-FMR	Isolated rat heart [50]	Rat [45, 46, 50, 51]	Rat [45, 51] Dog [45]	Dog [45]	Rat [45, 50, 51]	

responses to pharmacologic blocking by desipramine. Recently, our research group directly compared the uptake kinetics of these tracers in rabbit hearts [38]. As expected, desipramine pre-treatment significantly inhibited heart uptake of ^{123}I–MIBG, ^{11}C–HED, and ^{18}F–LMI1195 in the same manner. However, when desipramine treatment was undertaken 10 min after tracer injection (namely desipramine chase), the retention kinetics of ^{123}I–MIBG and ^{18}F–LMI1195 did not change, whereas ^{11}C–HED washout increased significantly (Fig. 3). These findings can be attributed to the different mechanism of accumulation of these tracers: It can be hypothesized that ^{123}I–MIBG and ^{18}F–LMI1195 are stored stably in synaptic vesicles. Thus, after entering synaptic vesicles, they will not be affected by the uptake-1 mechanism inhibitors anymore. Nevertheless, it can be presumed that ^{11}C–HED maintains a dynamic equilibrium through repeated release from and reabsorption into nerve terminals (Fig. 3).

In vivo studies in rats, rabbits, and cynomolgus monkeys demonstrated high and sustained cardiac uptake of ^{18}F–LMI1195 continuously over 120 min after injection. The specificity of ^{18}F–LMI1195 for uptake-1 mechanism was confirmed also in rabbits and cynomolgus monkeys [32]. Furthermore, in comparison with ^{123}I–MIBG, ^{18}F–LMI1195 is washed out more rapidly from non-target organs such as blood, lung, and liver, resulting in significantly higher heart-to-background ratios with clear cardiac images [32]. In cynomolgus monkeys, heart-to-liver uptake ratios of ^{18}F–LMI1195 were more than three times higher than ^{123}I–MIBG (3.5 versus 1.1) at 30 min after injection. Of note, the transport system involved in ^{18}F–LMI1195 uptake is not identical in different species. In addition to uptake-1 mechanism, there is a second way to take up endogenous neurotransmitter or radiotracer into non-neuronal tissue, namely uptake-2 mechanism. Unlike in rabbits and nonhuman primate hearts, a similar blocking effect by desipramine has not been observed in rat hearts. Our research group revealed that phenoxybenzamine, a nonselective blocker of both uptake-1 and uptake-2

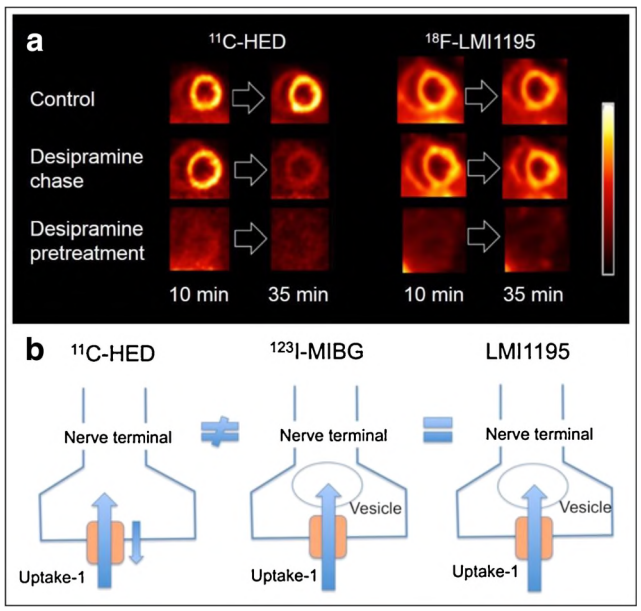

Fig. 3 (A) Distinct blocking effect of desipramine on rabbit cardiac uptake of ^{11}C–HED and ^{18}F–LMI1195. (B) A conceptual model of the accumulation of ^{11}C–HED, ^{123}I–MIBG, and ^{18}F–LMI1195 after transportation into nerve terminal via uptake-1. Modified from Werner et al. (35) © by the Society of Nuclear Medicine and Molecular Imaging, Inc.

mechanisms, evidently inhibits ^{18}F–LMI1195 uptake in rat hearts, whereas desipramine failed [37]. A subsequent study by Yu et al. supports this conclusion by demonstrating remarkable inhibition of ^{18}F–LMI1195 uptake with high selectivity in rabbits and cynomolgus monkey hearts instead of rat hearts when pretreated with desipramine [35]. It should be noted that, despite these, ^{11}C–HED uptake in the rat heart can be successfully inhibited by desipramine [52, 53]. The reason for this discrepancy between ^{11}C–HED and ^{18}F–LMI1195 has not been fully clarified yet.

^{18}F–LMI1195 showed potential for regional assessment in some sympathetic denervation models. ^{18}F–LMI1195 PET clearly showed the regional phenol-denervated area in a rabbit model, whereas the myocardial perfusion assessed by ^{18}F–flurpiridaz PET was normal [33]. A later report by the same group also demonstrated decreased cardiac ^{18}F–LMI1195 uptake in 6-hydroxydoparmine (6-OHDA) denervated rabbit model [35].

A phase 1 clinical trial confirmed that ^{18}F–LMI1195 is well tolerated and exhibits a favorable biodistribution for cardiac imaging with acceptable radiation doses [39]. Twelve healthy subjects were administered 150–250 MBq of ^{18}F–LMI1195, and no safety concerns were observed during the study. A rapid clearance from the blood could be observed along with delineated clear cardiac uptake distributing evenly throughout the heart (Fig. 4). Furthermore, as derived from dynamic PET images, heart-to-lung and heart-to-liver ratios remained high over 5 h after injection. Although the largest peak uptakes were observed in the urinary bladder and the liver, it was concluded that accumulated radioactivity in the liver does not seem to affect the assessment of myocardial conditions in most cases. The mean effective dose of ^{18}F–LMI1195 was similar to that previously reported for ^{123}I–MIBG. Noteworthy, in healthy subjects, the metabolism of ^{18}F–LMI1195 in blood is rapid with ratios of 36.5%, 12.5%, and 7.2% of the parent compound in plasma samples at 15, 30, and 120 min after injection, respectively [39].

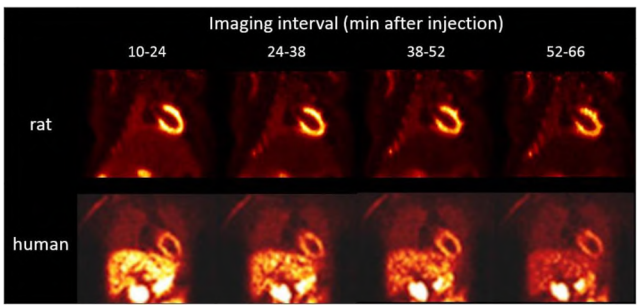

Fig. 4 Biodistribution of ^{18}F–LMI1195 in a healthy rat and a healthy subject. Modified from Sinusas et al. (40) and original data. © by the Society of Nuclear Medicine and Molecular Imaging, Inc.

^{18}F–4F-MHPG

The ^{18}F-labeled PET tracer 4-^{18}F-fluoro-3-hydroxyphenethylguanidine (^{18}F–4F-MHPG) was designed to provide properties of slow cardiac uptake and long retention, intending to reflect mild differences of sympathetic nervous status while excluding the blood flow effect [54]. Raffel and co-workers pointed out if a tracer shows rapid uptake into neuronal tissues by uptake-1 mechanism after its initial extraction from plasma, such as ^{11}C–HED and ^{123}I–MIBG, the neuronal uptake should largely depend upon blood flow. In that case, the rate constant for NET transportation (k3, the transportation from extracellular space to neuron compartment) should be much higher than the rate constant for washout (k2, the clearance from extracellular space back to plasma), which leads to a problem in using kinetic analysis techniques for the measurement of the regional nerve density. To overcome this problem, they set out to find the compound with slow neuronal uptake and long neuronal retention. As a result, ^{11}C–labeled compounds with a phenethylguanidine-like structure were screened and ^{11}C-4F-MHPG was found to fulfill the criteria [54]. Encouraged by the result achieved from ^{11}C-4F-MHPG, a corresponding ^{18}F-labeled 4F–MHPG was subsequently developed and evaluated [40]. Recently, its isomer 3-^{18}F-fluoro-4-hydroxyphenethylguanidine (^{18}F–3F-PHPG) has also been introduced. According to the latest article, radiosynthesis of these ^{18}F-labeled tracers can be prepared by ^{18}F fluorination and deprotection steps, using automated radiolabeling systems. The total synthesis time is 90 min, and decay-corrected yields of ^{18}F–4F-MHPG and ^{18}F–3F-PHPG are 7.0% and 8.0%, respectively [43].

^{18}F–4F-MHPG and ^{18}F–3F-PHPG were taken up slower than ^{11}C-labeled MIBG and ^{11}C–HED in isolated rat hearts, in which uptake-2 mechanism was pharmacologically blocked. The neuronal uptake rates of ^{18}F–4F-MHPG, ^{18}F–3F-PHPG, ^{11}C–MIBG, and ^{11}C–HED are 0.77, 0.79, 3.65, and 2.35 mL/min/g, respectively [43]. Furthermore, ^{18}F–4F-MHPG and ^{18}F–3F-PHPG demonstrated much longer retention than ^{11}C–MIBG and ^{11}C–HED in isolated heart [41, 43], which suggests ^{18}F–4F-MHPG and ^{18}F–3F-PHPG are stably stored in storage vesicles in neuronal terminals.

In vivo biodistribution studies of ^{18}F–4F-MHPG in rats exhibited favorable uptake in the heart and low uptake in the lungs and liver [40]. From the biodistribution data, the effective dose of ^{18}F–4F-MHPG for humans was estimated and considered as being acceptable for human use.

PET imaging with ^{18}F–4F-MHPG and ^{18}F–3F-PHPG in a rhesus macaque monkey demonstrated clear and sustained myocardial uptake throughout 90 min. It should be noted that the clearance of ^{18}F–4F-MHPG from the liver was faster, providing a higher heart-to-liver ratio at 85 min after injection, compared to ^{18}F–3F-PHPG (2.5 vs. 2.2) [41, 43]. ^{18}F–4F-MHPG showed high specificity to uptake-1 mechanism in

pharmacologic blocking study using rhesus macaque monkey. Additionally, "net uptake rate" constant for each compound could be calculated by either compartmental modeling or Patlak graphical analysis. Moreover, desipramine pre-treatment decreased "net uptake rate" constant for ^{18}F–4F-MHPG in a dose-dependent manner. These results suggest that either compound has optimal kinetics, which can be applied to the kinetic analysis approaches, and provide quantitative values that are sensitive to mild or regional denervation [41, 43]. In vivo metabolite analysis in monkey revealed that ^{18}F–4F-MHPG is metabolized more rapidly than ^{18}F–3F-PHPG: The time needed for 50% metabolism were 2.3 min for ^{18}F–4F-MHPG and 6.7 min for ^{18}F–3F-PHPG. Metabolic processes of these tracers do not seem to be identical because only ^{18}F–4F-MHPG is metabolized while incubated with monkey liver cytosol fractions [41, 43].

Recently, first-in-human studies have been performed focusing on basic biodistribution in human and myocardial kinetic analysis [42]. It has been revealed that, in normal human subjects, both tracers successfully yielded clear cardiac images and quantitative measures of regional nerve density along with negligible lung uptake and reasonably low liver uptake. Consistent with animal PET imaging, ^{18}F–4F-MHPG was cleared from the liver more rapidly to generate a better heart-to-liver ratio. On the other hand, ^{18}F–3F-PHPG showed higher cardiac uptake and slow metabolism. More information regarding these two tracers might open the window for future clinical application together with new ideas for better tracer design.

Advantages of the novel ^{18}F-labeld tracers over conventional tracers

The novel ^{18}F-labeled PET tracers reviewed here have a potential to provide more detailed information of sympathetic nervous status including regional and absolute assessment in routine clinical practice.

Compared to ^{123}I–MIBG, all of these ^{18}F-labeled tracers yielded much better cardiac images due to higher resolution of PET techniques. Furthermore, optimized kinetics of these tracers could provide high heart-to-lung and heart-to-liver ratios, minimizing background uptake. Promising imaging quality of ^{18}F-labeled tracers emphasizes its potency of performing regional sympathetic nerve assessment, while the significance of which has been shown using ^{11}C–HED as mentioned above. Unlike ^{11}C-labeled tracers, ^{18}F-labeled tracers have a potential to be used widely, at relatively low cost, by using established commercial network of PET tracers.

All of the three ^{18}F-labeled tracers have unique kinetics. However, the accumulated information of conventional sympathetic nervous imaging might be easily applied to ^{18}F–LMI1195 imaging because it has relatively similar kinetics as MIBG than other two compounds. Optimization of quantitative parameter would be the subject of future investigations. On the other hand, ^{18}F–4F-MHPG and ^{18}F–3F-PHPG seem to have the favorable properties for absolute quantification, although the establishment of quantification methods would be needed.

Conclusion

Novel ^{18}F-labeled PET tracers, which have been developed after the successful clinical implementation of the radiotracers ^{123}I–MIBG and ^{11}C–HED, may largely change the future of myocardial sympathetic nervous imaging. The potentials of ^{18}F-labeled tracers are based on the long-term contributions of ^{123}I–MIBG and ^{11}C–HED imaging to establish the significance of radionuclide sympathetic nervous imaging. ^{18}F-labeled tracers can not only expand the availability of myocardial sympathetic nervous imaging, but also improve the flexibility of scan protocols and mitigate the financial burden of hospitals. Especially ^{18}F–LMI1195 and ^{18}F–4F-MHPG have already been proven to possess favorable properties for cardiac imaging in humans.

Certainly, novel insights about ^{18}F-labeled tracers in human subjects are essential for clinical use. In the meantime, further investigations of the detailed mechanism of ^{18}F-labeled tracer uptake are also necessary to design novel clinical imaging protocols and help in interpreting imaging results more properly.

So far, there has been no direct comparison of the mechanism or the performance of these tracers. Therefore, it is difficult to conclude which tracer has the best property for clinical application, especially with regard to regional assessment or quantification of sympathetic nervous activity. Further characterization of these tracers would be of utmost importance.

^{123}I–MIBG, ^{123}I–meta-iodobenzylguanidine; SPECT, single photon emission computed tomography; PET, positron emission tomography; HF, heart failure; NET, norepinephrine transporters; ADMIRE-HF, AdreView Myocardial Imaging for Risk Evaluation in Heart Failure; LVEF, left ventricular ejection fractio; H/M, heart-to-mediastinum; BNP, B-type natriuretic peptide; SCD, sudden cardiac death; EPI, epinephrine; PHEN, phenylephrine; HED, hydroxyephedrine; MAO, monoamine oxidase; CPAP, continuous positive airway pressure; HFrEF, HF with reduced ejection fraction; FDG, fluorodeoxyglucose; 6-OHDA, 6-hydroxydoparmine

Funding This research received no specific grant from any funding agency in the public, commercial, or not-for-profit sectors.

Compliance with ethical standards

Conflict of interest The authors declare that they have no conflict of interest.

Ethical approval This article does not contain any studies with human participants or animals performed by any of the authors.

References

1. Zhang DY, Anderson AS. The sympathetic nervous system and heart failure. Cardiol Clin. 2014;32(1):33–45, **vii**. https://doi.org/10.1016/j.ccl.2013.09.010.
2. Packer M, Bristow MR, Cohn JN, Colucci WS, Fowler MB, Gilbert EM, et al. The effect of carvedilol on morbidity and mortality in patients with chronic heart failure. U.S. Carvedilol heart failure study group. N Engl J Med. 1996;334(21):1349–55. https://doi.org/10.1056/nejm199605233342101.
3. Lancet. The cardiac insufficiency Bisoprolol study II (CIBIS-II): a randomised trial. Lancet. 1999;353(9146):9–13.
4. Goldstein S, Hjalmarson A. The mortality effect of metoprolol CR/XL in patients with heart failure: results of the MERIT-HF trial. Clin Cardiol. 1999;22(Suppl 5):V30–5.
5. Wollenweber T, Bengel FM. Cardiac molecular imaging. Semin Nucl Med. 2014;44(5):386–97. https://doi.org/10.1053/j.semnuclmed.2014.05.002.
6. Boogers MJ, Fukushima K, Bengel FM, Bax JJ. The role of nuclear imaging in the failing heart: myocardial blood flow, sympathetic innervation, and future applications. Heart Fail Rev. 2011;16(4):411–23. https://doi.org/10.1007/s10741-010-9196-0.
7. Carrio I, Cowie MR, Yamazaki J, Udelson J, Camici PG. Cardiac sympathetic imaging with mIBG in heart failure. JACC Cardiovasc Imag. 2010;3(1):92–100. https://doi.org/10.1016/j.jcmg.2009.07.014.
8. Marwick TH, Raman SV, Carrio I, Bax JJ. Recent developments in heart failure imaging. JACC Cardiovasc Imag. 2010;3(4):429–39. https://doi.org/10.1016/j.jcmg.2010.02.002.
9. Eckelman WC, Dilsizian V. Chemistry and biology of radiotracers that target changes in sympathetic and parasympathetic nervous systems in heart disease. J Nucl Med : Off Publ, Soc Nucl Med. 2015;56(Suppl 4):7s–10s. https://doi.org/10.2967/jnumed.114.142802.
10. Flotats A, Carrio I. Cardiac neurotransmission SPECT imaging. J Nucl Cardiol : Off Publ Am Soc Nucl Cardiol. 2004;11(5):587–602. https://doi.org/10.1016/j.nuclcard.2004.07.007.
11. Henderson EB, Kahn JK, Corbett JR, Jansen DE, Pippin JJ, Kulkarni P, et al. Abnormal I-123 metaiodobenzylguanidine myocardial washout and distribution may reflect myocardial adrenergic derangement in patients with congestive cardiomyopathy. Circulation. 1988;78(5 Pt 1):1192–9.
12. Wakabayashi T, Nakata T, Hashimoto A, Yuda S, Tsuchihashi K, Travin MI, et al. Assessment of underlying etiology and cardiac sympathetic innervation to identify patients at high risk of cardiac death. J Nucl Med. 2001;42(12):1757–67.
13. Dimitriu-Leen AC, Scholte AJ, Jacobson AF. 123I–MIBG SPECT for Evaluation of Patients with Heart Failure. Journal of nuclear medicine : official publication, Society of Nuclear Medicine. 2015;56 Suppl 4:25s–30s. doi:https://doi.org/10.2967/jnumed.115.157503.
14. Merlet P, Valette H, Dubois-Rande JL, Moyse D, Duboc D, Dove P, et al. Prognostic value of cardiac metaiodobenzylguanidine imaging in patients with heart failure. J Nucl Med : Off Publ, Soc Nucl Med. 1992;33(4):471–7.
15. Verberne HJ, Brewster LM, Somsen GA, van Eck-Smit BL. Prognostic value of myocardial 123I-metaiodobenzylguanidine (MIBG) parameters in patients with heart failure: a systematic review. Eur Heart J. 2008;29(9):1147–59. https://doi.org/10.1093/eurheartj/ehn113.
16. Nakata T, Miyamoto K, Doi A, Sasao H, Wakabayashi T, Kobayashi H, et al. Cardiac death prediction and impaired cardiac sympathetic innervation assessed by MIBG in patients with failing and nonfailing hearts. J Nucl Cardiol : Off Publ Am Soc Nucl Cardiol. 1998;5(6):579–90.
17. Jacobson AF, Senior R, Cerqueira MD, Wong ND, Thomas GS, Lopez VA, et al. Myocardial Iodine-123 meta-Iodobenzylguanidine imaging and cardiac events in heart FailureResults of the prospective ADMIRE-HF (AdreView myocardial imaging for risk evaluation in heart failure) study. J Am Coll Cardiol. 2010;55(20):2212–21. https://doi.org/10.1016/j.jacc.2010.01.014.
18. Nakajima K, Nakata T, Matsuo S, Jacobson AF. Creation of mortality risk charts using 123I meta-iodobenzylguanidine heart-to-mediastinum ratio in patients with heart failure: 2- and 5-year risk models. Eur Heart J Cardiovasc Imag. 2016;17(10):1138–45. https://doi.org/10.1093/ehjci/jev322.
19. Tamaki S, Yamada T, Okuyama Y, Morita T, Sanada S, Tsukamoto Y, et al. Cardiac iodine-123 metaiodobenzylguanidine imaging predicts sudden cardiac death independently of left ventricular ejection fraction in patients with chronic heart failure and left ventricular systolic dysfunction: results from a comparative study with signal-averaged electrocardiogram, heart rate variability, and QT dispersion. J Am Coll Cardiol. 2009;53(5):426–35. https://doi.org/10.1016/j.jacc.2008.10.025.
20. Bardy GH, Lee KL, Mark DB, Poole JE, Packer DL, Boineau R, et al. Amiodarone or an implantable cardioverter-defibrillator for congestive heart failure. N Engl J Med. 2005;352(3):225–37. https://doi.org/10.1056/NEJMoa043399.
21. Kelesidis I, Travin MI. Use of cardiac radionuclide imaging to identify patients at risk for arrhythmic sudden cardiac death. J Nucl Cardiol : Off Publ Am Soc Nucl Cardiol. 2012;19(1):142–152; **quiz 53-7**. https://doi.org/10.1007/s12350-011-9482-9.
22. Kawai T, Yamada T, Tamaki S, Morita T, Furukawa Y, Iwasaki Y, et al. Usefulness of cardiac meta-iodobenzylguanidine imaging to identify patients with chronic heart failure and left ventricular ejection fraction <35% at low risk for sudden cardiac death. Am J Cardiol. 2015;115(11):1549–54. https://doi.org/10.1016/j.amjcard.2015.02.058.
23. Travin MI. Current clinical applications and next steps for cardiac Innervation imaging. Curr Cardiol Rep. 2017;19(1):1. https://doi.org/10.1007/s11886-017-0817-2.
24. Boutagy NE, Sinusas AJ. Recent advances and clinical applications of PET cardiac autonomic nervous system imaging. Curr Cardiol Rep. 2017;19(4):33. https://doi.org/10.1007/s11886-017-0843-0.
25. Lautamaki R, Sasano T, Higuchi T, Nekolla SG, Lardo AC, Holt DP, et al. Multiparametric molecular imaging provides mechanistic insights into sympathetic innervation impairment in the viable infarct border zone. J Nucl Med : Off Publ, Soc Nucl Med. 2015;56(3):457–63. https://doi.org/10.2967/jnumed.114.149971.
26. Bravo PE, Lautamaki R, Carter D, Holt DP, Nekolla SG, Dannals RF, et al. Mechanistic insights into sympathetic neuronal regeneration: multitracer molecular imaging of catecholamine handling after cardiac transplantation. Circ Cardiovasc Imag. 2015;8(8):e003507. https://doi.org/10.1161/circimaging.115.003507.
27. Boschi S, Lodi F, Boschi L, Nanni C, Chondrogiannis S, Colletti PM, et al. 11C-Meta-hydroxyephedrine: a promising PET radiopharmaceutical for imaging the sympathetic nervous system. Clin

Nucl Med. 2015;40(2):e96–e103. https://doi.org/10.1097/rlu.0000000000000512.
28. Hall AB, Ziadi MC, Leech JA, Chen SY, Burwash IG, Renaud J, et al. Effects of short-term continuous positive airway pressure on myocardial sympathetic nerve function and energetics in patients with heart failure and obstructive sleep apnea: a randomized study. Circulation. 2014;130(11):892–901. https://doi.org/10.1161/circulationaha.113.005893.
29. Fallavollita JA, Heavey BM, Luisi AJ Jr, Michalek SM, Baldwa S, Mashtare TL Jr, et al. Regional myocardial sympathetic denervation predicts the risk of sudden cardiac arrest in ischemic cardiomyopathy. J Am Coll Cardiol. 2014;63(2):141–9. https://doi.org/10.1016/j.jacc.2013.07.096.
30. Fujita W, Matsunari I, Aoki H, Nekolla SG, Kajinami K. Prediction of all-cause death using 11C-hydroxyephedrine positron emission tomography in Japanese patients with left ventricular dysfunction. Ann Nucl Med. 2016; https://doi.org/10.1007/s12149-016-1081-z.
31. Ducharme J, Goertzen AL, Patterson J, Demeter S. Practical aspects of 18F-FDG PET when receiving 18F-FDG from a distant supplier. J Nucl Med Technol. 2009;37(3):164–9. https://doi.org/10.2967/jnmt.109.062950.
32. Yu M, Bozek J, Lamoy M, Guaraldi M, Silva P, Kagan M, et al. Evaluation of LMI1195, a novel 18F-labeled cardiac neuronal PET imaging agent, in cells and animal models. Circ Cardiovasc Imag. 2011;4(4):435–43. https://doi.org/10.1161/CIRCIMAGING.110.962126.
33. Yu M, Bozek J, Lamoy M, Kagan M, Benites P, Onthank D, et al. LMI1195 PET imaging in evaluation of regional cardiac sympathetic denervation and its potential role in antiarrhythmic drug treatment. Eur J Nucl Med Mol Imaging. 2012;39(12):1910–9. https://doi.org/10.1007/s00259-012-2204-y.
34. Higuchi T, Yousefi BH, Reder S, Beschorner M, Laitinen I, Yu M, et al. Myocardial kinetics of a novel [(18)F]-labeled sympathetic nerve PET tracer LMI1195 in the isolated Perfused rabbit heart. JACC Cardiovasc Imag. 2015;8(10):1229–31. https://doi.org/10.1016/j.jcmg.2014.11.013.
35. Yu M, Bozek J, Kagan M, Guaraldi M, Silva P, Azure M, et al. Cardiac retention of PET neuronal imaging agent LMI1195 in different species: impact of norepinephrine uptake-1 and -2 transporters. Nucl Med Biol. 2013;40(5):682–8. https://doi.org/10.1016/j.nucmedbio.2013.03.003.
36. Gaertner FC, Wiedemann T, Yousefi BH, Lee M, Repokis I, Higuchi T, et al. Preclinical evaluation of 18F-LMI1195 for in vivo imaging of pheochromocytoma in the MENX tumor model. J Nucl Med : Off Publ, Soc Nucl Med. 2013;54(12):2111–7. https://doi.org/10.2967/jnumed.113.119966.
37. Higuchi T, Yousefi BH, Kaiser F, Gartner F, Rischpler C, Reder S, et al. Assessment of the 18F-labeled PET tracer LMI1195 for imaging norepinephrine handling in rat hearts. J Nucl Med : Off Publ, Soc Nucl Med. 2013;54(7):1142–6. https://doi.org/10.2967/jnumed.112.104232.
38. Werner RA, Rischpler C, Onthank D, Lapa C, Robinson S, Samnick S, et al. Retention kinetics of the 18F-labeled sympathetic nerve PET tracer LMI1195: comparison with 11C-Hydroxyephedrine and 123I-MIBG. J Nucl Med : Off Publ, Soc Nucl Med. 2015;56(9):1429–33. https://doi.org/10.2967/jnumed.115.158493.
39. Sinusas AJ, Lazewatsky J, Brunetti J, Heller G, Srivastava A, Liu YH, et al. Biodistribution and radiation dosimetry of LMI1195: first-in-human study of a novel 18F-labeled tracer for imaging myocardial innervation. J Nucl Med : Off Publ, Soc Nucl Med. 2014;55(9):1445–51. https://doi.org/10.2967/jnumed.114.140137.
40. Jang KS, Jung YW, Sherman PS, Quesada CA, Gu G, Raffel DM. Synthesis and bioevaluation of [(18)F]4-fluoro-m-hydroxyphenethylguanidine ([(18)F]4F-MHPG): a novel radiotracer for quantitative PET studies of cardiac sympathetic innervation. Bioorg Med Chem Lett. 2013;23(6):1612–6. https://doi.org/10.1016/j.bmcl.2013.01.106.
41. Jang KS, Jung YW, Gu G, Koeppe RA, Sherman PS, Quesada CA, et al. 4-[18F]Fluoro-m-hydroxyphenethylguanidine: a radiopharmaceutical for quantifying regional cardiac sympathetic nerve density with positron emission tomography. J Med Chem. 2013;56(18):7312–23. https://doi.org/10.1021/jm400770g.
42. Raffel D, Jung Y-W, Murthy V, Gu G, Rothley J, Koeppe R et al. First-in-human studies of 18F–hydroxyphenethylguanidines: PET radiotracers for quantifying cardiac sympathetic nerve density. Journal of Nuclear Medicine. 2016;57(supplement 2):232.
43. Jung Y-W, Jang KS, Gu G, Koeppe RA, Sherman PS, Quesada CA et al. [18F] Fluoro-Hydroxyphenethylguanidines: Efficient Synthesis and Comparison of Two Structural Isomers as Radiotracers of Cardiac Sympathetic Innervation. ACS Chemical Neuroscience. 2017.
44. Vaidyanathan G, McDougald D, Koumarianou E, Choi J, Hens M, Zalutsky MR. Synthesis and evaluation of 4-[18F]fluoropropoxy-3-iodobenzylguanidine ([18F]FPOIBG): a novel 18F-labeled analogue of MIBG. Nucl Med Biol. 2015;42(8):673–84. https://doi.org/10.1016/j.nucmedbio.2015.04.005.
45. Langer O, Valette H, Dolle F, Halldin C, Loc'h C, Fuseau C, et al. High specific radioactivity (1R,2S)-4-[(18)F]fluorometaraminol: a PET radiotracer for mapping sympathetic nerves of the heart. Nucl Med Biol. 2000;27(3):233–8.
46. Langer O, Dolle F, Valette H, Halldin C, Vaufrey F, Fuseau C, et al. Synthesis of high-specific-radioactivity 4- and 6-[18F]fluorometaraminol-PET tracers for the adrenergic nervous system of the heart. Bioorg Med Chem. 2001;9(3):677–94.
47. Wieland DM, Rosenspire KC, Hutchins GD, Van Dort M, Rothley JM, Mislankar SG, et al. Neuronal mapping of the heart with 6-[18F]fluorometaraminol. J Med Chem. 1990;33(3):956–64.
48. Mislankar SG, Gildersleeve DL, Wieland DM, Massin CC, Mulholland GK, Toorongian SA. 6-[18F]Fluorometaraminol: a radiotracer for in vivo mapping of adrenergic nerves of the heart. J Med Chem. 1988;31(2):362–6.
49. Rosenspire KC, Gildersleeve DL, Massin CC, Mislankar SG, Wieland DM. Metabolic fate of the heart agent [18F]6-fluorometaraminol. Int J Rad Appl Instrum B. 1989;16(7):735–9.
50. Pissarek M, Ermert J, Oesterreich G, Bier D, Coenen HH. Relative uptake, metabolism, and beta-receptor binding of (1R,2S)-4-(18)F-fluorometaraminol and (123)I-MIBG in normotensive and spontaneously hypertensive rats. J Nucl Med : Off Publ, Soc Nucl Med. 2002;43(3):366–73.
51. Eskola O, Gronroos T, Bergman J, Haaparanta M, Marjamaki P, Lehikoinen P, et al. A novel electrophilic synthesis and evaluation of medium specific radioactivity (1R, 2S)-4-[18F]fluorometaraminol, a tracer for the assessment of cardiac sympathetic nerve integrity with PET. Nucl Med Biol. 2004;31(1):103–10.
52. Rischpler C, Fukushima K, Isoda T, Javadi MS, Dannals RF, Abraham R, et al. Discrepant uptake of the radiolabeled norepinephrine analogues hydroxyephedrine (HED) and metaiodobenzylguanidine (MIBG) in rat hearts. Eur J Nucl Med Mol Imaging. 2013;40(7):1077–83. https://doi.org/10.1007/s00259-013-2393-z.
53. DeGrado TR, Hutchins GD, Toorongian SA, Wieland DM, Schwaiger M. Myocardial kinetics of carbon-11-meta-hydroxyephedrine: retention mechanisms and effects of norepinephrine. J Nucl Med : Off Publ, Soc Nucl Med. 1993;34(8):1287–93.
54. Raffel DM, Jung YW, Gildersleeve DL, Sherman PS, Moskwa JJ, Tluczek LJ, et al. Radiolabeled phenethylguanidines: novel imaging agents for cardiac sympathetic neurons and adrenergic tumors. J Med Chem. 2007;50(9):2078–88. https://doi.org/10.1021/jm061398y.